



Methane Conversion Under Mild Conditions Using Semiconductors and Metal-Semiconductors as Heterogeneous Photocatalysts: State of the Art and Challenges

*Eliane Ribeiro Januario, Patrícia Ferreira Silvaino, Arthur Pignataro Machado, Jorge Moreira Vaz and Estevam Vitorio Spinace**

Instituto de Pesquisas Energéticas e Nucleares – IPEN-CNEN/SP, Centro de Células a Combustível e Hidrogênio, Cidade Universitária, São Paulo, Brazil

OPEN ACCESS

Edited by:

Jose Maria Bueno,
Federal University of São Carlos, Brazil

Reviewed by:

Vincenzo Vaiano,
University of Salerno, Italy
Dalmo Mandelli,
Federal University of ABC, Brazil

*Correspondence:

Estevam Vitorio Spinace
espinace@ipen.br

Specialty section:

This article was submitted to
Catalysis and Photocatalysis,
a section of the journal
Frontiers in Chemistry

Received: 24 March 2021

Accepted: 17 June 2021

Published: 30 June 2021

Citation:

Januario ER, Silvaino PF, Machado AP,
Moreira Vaz J and Spinace EV (2021)
Methane Conversion Under Mild
Conditions Using Semiconductors
and Metal-Semiconductors as
Heterogeneous Photocatalysts: State
of the Art and Challenges.
Front. Chem. 9:685073.
doi: 10.3389/fchem.2021.685073

The processes currently used in the chemical industry for methane conversion into fuels and chemicals operate under extreme conditions like high temperatures and pressures. In this sense, the search for methane conversion under mild conditions remains a great challenge. This review aims to summarize the use semiconductors and metal-semiconductors as heterogeneous photocatalysts for methane conversion under mild conditions into valuable products. First, a brief presentation of photochemical conversion of methane is provided and then the focus of this review on the use of heterogeneous photocatalysts for methane conversion are described. Finally, the main challenges and opportunities are discussed.

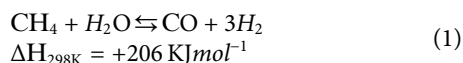
Keywords: methane, photocatalysts, heterogeneous, semiconductor, metal-semiconductor

INTRODUCTION

Methane is the principal component of natural gas having the highest C/H ratio among the hydrocarbons and is an important source of carbon (C₂₊), carbon monoxide and hydrogen for the chemical industry (Horn and Schlögl, 2015; Olivos-Suarez et al., 2016). However, methane is one of the most stable molecule and methane conversions are thermodynamically unfavorable at 298°K due to the positive and large value of the Gibbs free energy of formation ($\Delta G > 0$). Thus, high reaction temperatures are required to transform methane into more valuable and useful chemicals and to promote such reactions suitable catalysts are also necessary to reduce the activation energy (Yuliati and Yoshida, 2008). In this manner, further development of technology for methane conversion under mild conditions in order to reduce the energy consumption and the environmental impacts are highly desired (Horn and Schlögl, 2015; Olivos-Suarez et al., 2016).

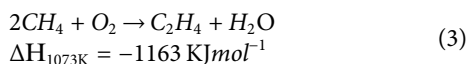
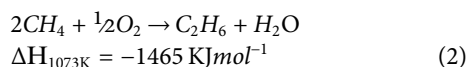
THERMOCATALYTIC CONVERSION OF METHANE

The steam reforming of methane (SRM) is the main process currently used for hydrogen and carbon monoxide production (Eq. 1), which are key intermediates in the chemical industry. This reaction is endothermic and the catalytic process is carried in the temperature range of 970–1100°K and pressure up to 3.5 MPa (Horn and Schlögl, 2015; Olivos-Suarez et al., 2016).



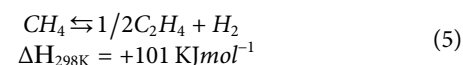
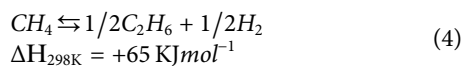
The methane steam reforming reaction is an indirect route for transforming methane into higher value-added chemicals such as ammonia, methanol and liquid fuels.

A direct route of high industrial interest is the oxidative coupling of methane (OCM) to ethane and ethylene (Eqs 2, 3). This is a highly exothermic reaction and occurs in the presence of several metal oxide catalysts at temperatures between 773 and 1273 K (Olivos-Suarez et al., 2016; Gao et al., 2019).



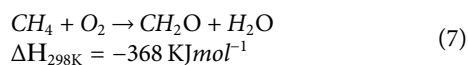
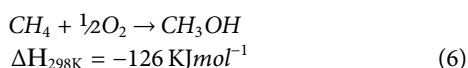
The main products of these reactions are ethane and ethene in addition to CO₂ and CO, but due to difficult control of this process it was not industrially applied yet (Horn and Schlögl, 2015; Olivos-Suarez et al., 2016).

In the non-oxidative coupling of methane (NOMC), methane is directly converted into ethane and/or ethylene and hydrogen (Eqs 4, 5) in the presence of a catalyst (Zeng et al., 2018).



However, the two-stage process taking place at different temperatures is difficult to operate and the thermodynamic limitations cause extremely low activity (Tang et al., 2014).

Another direct route of high industrial interest is the direct oxidation of methane to methanol (Eq. 6) and/or formaldehyde (Eq. 7) using heterogeneous catalysts (Song et al., 2019a).



In this case, although the reactions are thermodynamically favored, they are also difficult to control because the products formed are more reactive than methane leading to over-oxidation products, mainly CO₂. Thus, despite decades of research partial oxidation reactions of methane and oxygen are yet difficult to control and both are even further away from practical applications (Horn and Schlögl, 2015; Olivos-Suarez et al., 2016).

PHOTOCATALYTIC CONVERSION OF METHANE

An alternative to minimize energy use and environmental impacts is to perform the methane conversions at milder temperatures and under conditions that are easier to control, which is possible using photoenergy instead of the thermal energy. Photochemical reactions proceed at low temperatures because the photoenergy surpasses the activation energy of the chemical reactions (Yuliati and Yoshida, 2008). On the other hand, despite this photoenergy is

too low to break directly the C-H bond (434 kJ mol⁻¹) of methane, the use of photocatalysts may favor its activation at mild conditions in thermodynamically unfavorable reactions ($\Delta G > 0$) (Yuliati and Yoshida, 2008). For thermal catalytic reactions, the forward and backward reactions continue to occur at equilibrium while for photocatalytic reactions they can be considered as two different reactions requiring different energies and occurring by different mechanisms. Thus, the photocatalytic reaction break the thermodynamic equilibrium by decreasing or eliminating the backward reaction (Yuliati and Yoshida, 2008).

In the photocatalytic reactions, semiconductors are used as photocatalysts and when the photoenergy is greater than the band gap (E_g) of the semiconductor the photoexcitation occurs resulting in the promotion of an electron (e^-) from the valence band (VB) to the conduction band (CB) forming a hole (h^+) in the latter. The excited electrons and holes have potential enough to promote reduction and oxidation reactions (half reactions), respectively (Yuliati and Yoshida, 2008; Song et al., 2019b).

The photocatalysis involves a sequence of processes comprising the following steps: photon absorption, charge separation, charge carrier diffusion and transport, surface redox reactions, and reactant or product mass transfer. In order to obtain a good performance, all processes must take place efficiently (Takanabe, 2019). Thus, photocatalytic reaction is affected by the absorption of light, the separation and migration of electron-hole pairs and the chemical reaction on the catalyst surface and its efficiency can be improved by increasing the effective photon absorption, promoting charge separation and creating more active sites (Yuliati and Yoshida, 2008; Liu et al., 2017).

The photocatalytic non-oxidative coupling of methane at around room temperature was first described in 1998. Using TiO₂-SiO₂ and Ga₂O₃ as photocatalysts under UV irradiation it was possible to obtain ethane as the main product, however conversions were very low (Yuliati and Yoshida, 2008). The use of solar energy and a photocatalyst would also be an ideal method to produce hydrogen from water as an environmentally benign fuel (Shimura et al., 2010). However, this reaction has a positive value of Gibbs free energy ($\Delta G > 0$) which makes it difficult to occur. To circumvent this barrier, the a sacrificial reagent is used to consume the photogenerated holes reducing the reverse reactions (Shimura et al., 2010). Sacrificial reagents normally used were some kinds of carbon-related materials like sugar, starch, cellulose, coal and some compounds such as methanol, ethanol, ethylene and carbon monoxide. The production of hydrogen using methane as a “sacrificial reagent” was described by Yoshida and collaborators (Yoshida et al., 2007) in a reaction interpreted as a photocatalytic steam reforming of methane (PSRM), where Pt-loaded on semiconductors (NaTaO₃ and TiO₂) were used as photocatalysts to convert methane and water.

HETEROGENEOUS PHOTOCATALYSTS FOR METHANE CONVERSION

Although activation of methane using heterogeneous photocatalysts are quite interesting from the academic and

TABLE 1 | Methane conversion using semiconductors as photocatalysts arranged in the order of publication year.

Entry	Reactor	Source	Photocatalyst	Photocatalyst amount	CH ₄ inlet	H ₂ O	CH ₄ conv	t	T	Products formed	References
(1)	Closed quartz reaction vessel (82 ml)	Xe lamp 250 W	SiO ₂ .Al ₂ O ₃ spread on the flat bottom of the vessel	1.0 g	100 μmol (21 torr)	-	5.9%	18 h	310°K	C ₂ H ₆ (3.5) C ₂ H ₄ (0.4) C ₃ H ₈ (0.85) C ₃ H ₆ (0.3), μmol	Kato et al. (1998)
(2)	Closed quartz reactor (30 cm ³)	300 W Xe lamp	Ga ₂ O ₃	0.2 g	CH ₄ (200 μmol)	-	-	3 h	314°K	C ₂ H ₆ = 0.51 μmol C ₂ H ₄ = 0.01 μmol C ₃ H ₈ = 0.05 μmol H ₂ = 0.74 μmol	Yuliati et al. (2008a), Yuliati et al. (2008b)
(3)	Commercial photochemical reactor (Ace Glass)	Hg lamp 450 W	-β zeolite (BEA) -Bi-V- BEA	0.50 g L ⁻¹	CH ₄ /He (20%) ~22 ml min ⁻¹	300 ml	-	120 min	70°C	Bi-V-BEA CH ₃ OH = 11 μmol g ⁻¹ h ⁻¹ C ₂ H ₆ = 2.5 μmol g ⁻¹ h ⁻¹ CO ₂ = 150 μmol g ⁻¹ h ⁻¹ CO ₂	Murcia-López et al. (2017)
(4)	Home made fixed bed tubular quartz reactor 500 ml	Hg lamp 10 W	Ga ₂ O ₃ /AC (15 wt%)	0.20 g	CH ₄ :O ₂ :N ₂ 1.56 mmol L ⁻¹ CH ₄	-	91.5%	150 min	25°C	CO ₂	Wei et al. (2017)
(5)	Gas-tight glass cell	300-W Xe lamp	CeO ₂ treated 500–1,100°C	2 mg	0.2 bar CH ₄	15 ml	-	-	-	CH ₃ CHO = 1.0 μmol g ⁻¹ h ⁻¹ CH ₃ CH ₂ OH = 11.4 μmol g ⁻¹ h ⁻¹	Du et al. (2020)
(6)	Autoclave of 130 ml equipped with a quartz window	300 W Xenon lamp	TiO ₂ , Fe ₂ O ₃ , NiO, CuO, ZnO, WO ₃	20 mg	3 MPa CH ₄ and Fe ²⁺ /H ₂ O ₂ (Fenton)	20 ml	0.39%	1 h	30°C	Fenton/TiO ₂ CH ₃ OH = 471 μmol g ⁻¹ h ⁻¹ HCOOH = 34 μmol g ⁻¹ h ⁻¹ CH ₃ COH = 53 μmol g ⁻¹ h ⁻¹	Zeng et al. (2020)

technological point of view few papers have been published on the subject in the last years (Wu et al., 2021).

Semiconductor Photocatalysts

In this section the results of methane conversion using semiconductors as photocatalysts are presented (Table 1).

The non-oxidative coupling of methane proceeding under photoirradiation at around room temperature in the presence of silica-alumina as photocatalyst was first described in 1998 (Table 1, entry 1). It was detected C₂–C₄ alkanes in the gas phase and smaller amounts of C₂–C₆ alkanes and alkenes were detected after desorbing from the catalyst upon heating. It is important to highlight that CO and CO₂ were not detected and that in the absence of irradiation and/or catalysts, no products were observed. A 5.9% methane conversion was obtained after 18 h of irradiation resulting in an activity of 0.327 μmol h⁻¹ (Kato et al., 1998).

Yoshida and collaborators using gallium oxide (Ga₂O₃) converted photocatalytically methane mainly in ethane and

hydrogen at 314°K (Table 1, entry 2). It was observed that the conversion exceeded the equilibrium at this temperature indicating that Ga₂O₃ photocatalysts can selectively promote the forward reaction of the non-oxidative coupling of methane which is an advantage of the photocatalytic reaction (Yuliati et al., 2008a; Yuliati et al., 2008b).

Beta zeolite (H-BEA) was active for the oxidation of methane under UVC light) forming almost exclusively to CO₂ as the total oxidation product (Table 1, entry 3). The addition of V and Bi-V to the zeolite framework decreased the amount of acid sites due to the formation of V₂O₅ on the surface and improved the selectivity to less oxidized products. The addition of low Bi amount favored the formation of a BiVO₄/V₂O₅ heterojunction that acts as a visible light photocatalyst decreasing significantly the formation of CO₂ when compared to H-BEA and leading almost exclusively the formation of methanol instead of the ethylene formation (Murcia-López et al., 2017).

The photocatalytic decomposition of methane to CO₂ under UV irradiation was studied using β-Ga₂O₃ supported on activated

carbon (Table 1, entry 4). The photocatalytic activity was dependent on weight ratio of Ga₂O₃ being 15 wt% exhibited the best activity, which was more than sixfold of TiO₂ P25 benchmark photocatalyst. This increase of activity was ascribed to a strong adsorption capacity and improved separations of photoelectrons (e^-) and vacancies (h^+) pairs. The authors consider this method promising to remove low concentrations of methane (Wei et al., 2017).

Ceria nanoparticles with abundant oxygen vacancies were prepared at high temperatures under argon atmosphere, showing the highest oxygen vacancy concentration at 1,100°C (Table 1, entry 5). This material showed high activity for photocatalytic methane conversion leading to the formation of ethanol and acetaldehyde, being ethanol formed with 91.5% of selectivity. The aldehyde formation was attributed to the subsequent oxidation of the formed ethanol (Du et al., 2020).

The photocatalytic conversion of methane to oxygenated compounds at room temperature was studied combining the Fenton chemistry (Fe²⁺/H₂O₂) and different semiconductors like TiO₂, Fe₂O₃, NiO, CuO, ZnO and WO₃ (Table 1, entry 6). For comparative purposes, the Fenton reaction (FR), the traditional photocatalytic process (PCR) and the junction photo-Fenton reaction (PCFR) using TiO₂ as photocatalyst were performed. PCFR process showed the best results producing large amounts of methanol (up to 471 μmol g⁻¹ h⁻¹) with a selectivity of 83%, being the others products formic acid (HCOOH) and acetaldehyde (CH₃CHO). The semiconductors NiO, CuO and WO₃ also showed good methane conversions in the PCFR process; however producing HCOOH as the principal product with low selectivity values for methanol (in the range of 15–30%). Fe₂O₃ and ZnO showed low activities for methane conversion. The authors showed that the increase of PCFR process activity is a result of the synergism between Fenton reaction and photocatalysis involving active radicals (hydroxyl and superoxide) and charge carriers (excited electrons and holes) (Zeng et al., 2020).

Metal-Semiconductor Photocatalysts

Various studies have been shown that the integration of metals with semiconductors results in the formation of photocatalysts with improved activities that has been attributed to several factors: (Reddy et al., 2019; Wu et al., 2021).

- 1) the activation of methane by metals,
- 2) by displaying plasmonic oscillations that results in localized surface plasmon resonance (LSPR) effect,
- 3) to the improvement of charge separation (photoelectrons and holes) pulping the photoelectrons to surface for reactions (Schottky junction).

In Table 2 it was shown the use metal-semiconductor as photocatalysts for methane conversion.

Taylor considered the use of abundant and relatively low-cost reactants like light, water and methane was an attractive process to produce methanol and hydrogen (Table 2, entry 1). Using tungsten oxide (WO₃) doped with Pt, La or Cu and a mixture of CuLa as photocatalysts and an electron transfer reagent (methyl

viologen dichloride) at 370°K and 1.0 MPa it was possible to convert methane and water to methanol and hydrogen as the main products and ethane, oxygen, formic acid and carbon dioxide formed by side reactions. The tungsten oxide doped with lanthanum photocatalyst exhibited the largest methane conversion (~4%) and methanol yield of 1.7 g_{cat}⁻¹ h⁻¹ (Taylor, 2003).

The photocatalytic steam reforming of methane (PSRM) was performed around room temperature using doped and undoped Ga₂O₃ loaded with metals (Pt, Rh, Au, Pd and Ni) (Table 2, entry 2). The Pt/Ga₂O₃ exhibited superior performance for PSRM reaction exhibiting higher hydrogen production. The order of the activity was Pt > Rh > Au > Pd > Ni and the activity of the Pt/Ga₂O₃ photocatalyst was further enhanced by the addition of metal ions into the bulk and/or on the surface of Ga₂O₃. (Shimura et al., 2010).

The photoactivation of the methane C–H bond was performed using metal ions-modified ETS-10. This material is a microporous ordered titanosilicate with a framework containing one-dimensional O–Ti–O–Ti–O semiconducting nanowires (diameter of 0.67 nm) (Table 2, entry 3). These structures are insulated from one another by the surrounding SiO₂ matrix (Li et al., 2012). They considered that the combination of properties such quantum-confined titanate wires that improving the electron transfer, the uniform pore structure which allow the CH₄ access, and the presence of extra framework cations (Na⁺, K⁺), renders ETS-10 attractive for photoactivation applications. Besides this, the incorporation of extra metal ions into ETS-10 through either ion exchange or isomorphous substitution enhances its photoactivity. Through ion exchange it was prepared a series of metal ions-ETS-10 (metal ions = Ga³⁺, Al³⁺, Zn²⁺, Fe³⁺ and Cu²⁺). The photocatalysts were tested at room temperature for methane conversion in the absence of water and oxygen and C₂H₆ was the principal product formed with smaller amounts of C₂H₄ and C₃–C₄ alkanes and alkenes. Ga³⁺-ETS-10 showed the best activity and after 5 h of reaction a conversion of 14.9% was observed corresponding to a methane conversion of around 29.8 mmol g_{cat}⁻¹ h⁻¹. The authors associated the superior performance of Ga³⁺-ETS-10 to the presence of extraframework metal cations and the terminal Ti–OH groups on titanate wires, interacting with methane molecules under UV irradiation, leading to the cleavage of the methane C–H bond (Li et al., 2012).

The aqueous phase photocatalytic conversion of methane into methanol and hydrogen was investigated over Ag⁺-impregnated WO₃ (Table 2, entry 4). The characterization by different techniques showed that Ag⁺ ions shared surface oxygen with WO₃ forming Ag₂O that improved the photons absorption. The presence of cations Ag⁺ at the surface of semiconductor WO₃ enhanced the formation of •OH radicals and suppressed the charge carrier recombination process. On the other hand, the metal loading higher than 5% affect decrease the conversion process because photons are consumed preferentially in the dissociation of Ag₂O. The photocatalytic process occurred on the surface of the catalyst as well in the bulk that included water splitting and methanol formation. The measurement of evolved H₂ and O₂ in the gas phase and methanol in the liquid

TABLE 2 | Methane conversion using metal-semiconductors as photocatalysts arranged in the order of publication year.

Entry	Reactor	Source	Photocatalyst	Photocatalyst amount	CH ₄ inlet	H ₂ O	CH ₄ conv	t	T	Products formed	References
(1)	Commercial 1 L quartz	High pressure Hg lamp 350 W	WO ₃ doped with Pt, La or Cu	-	CH ₄ (5 ml min ⁻¹) 1.0 MPa pressure experiment, methyl viologen (MV) as electron transfer	750 ml	~4%	-	370°K	WO ₃ doped La CH ₃ OH = 1.7 g g ⁻¹ h ⁻¹	Taylor (2003)
(2)	Fixed-bed flow reactor - quartz cell (60 × 20 × 1 mm ³)	Xe lamp 300 W	Doped and undoped Ga ₂ O ₃ with Me (Pt,Rh, Au,Pd, Ni)	Catalyst (0.8 g) quartz granules (0.7 g)	H ₂ O _{vapour} (30 μmol min ⁻¹)/CH ₄ (120 μmol min ⁻¹) with Ar carrier (50 ml min ⁻¹)	Vapor	-	-	308°K	Pt/Ga ₂ O ₃ H ₂ = 0.55 μmol min ⁻¹	Shimura et al. (2010)
(3)	airtight quartz reactor (20 cm ³)	High pressure Hg lamp 150 W	Metal exchanged ETS-10	0.2 g spread on the wall of the reactor	200 μmol CH ₄	-	14.9%	5 h	RT	Ga ³⁺ ETS-10 C ₂ H ₆ ~20 mmol h ⁻¹ g ⁻¹	Li et al. (2012)
(4)	Self-fabricated photocatalytic reactor –batch process	Laser energy 100 MJ, 355 nm	5 wt% Ag ₂ O/WO ₃	0.30 g	100 ml/min for a period of 15 min after expelling oxygen by argon purging	70 ml	-	1.5 h	-	CH ₃ OH 13 μmol min ⁻¹ H ₂ ~ 42 μmol min ⁻¹	Hameed et al. (2014)
(5)	Quartz photochemical reactor (Ace Glass) of 500 ml	Medium-pressure mercury lamp (Ace Glass)–UV C	La doped mesoporous WO ₃	0.30 g	A mixture of methane (4.5 ml min ⁻¹) and helium (17.9 ml min ⁻¹) sparged continuously	300 ml	-	2 h	55°C	CH ₃ OH 9 μmol min ⁻¹ C ₂ H ₆ 1 μmol min ⁻¹ CO ₂ 10 μmol min ⁻¹	Villa et al. (2016)
(6)	Homemade fixed-bed pyrex reactor of 450 ml	Xe lamp 300 W, 200 mWcm ⁻²	Ag/ZnO (0.1 wt%)	0.50 g	95% N ₂ 5% CH ₄ 10 ml min ⁻¹ (free O ₂)	-	0.35%	-	RT	C ₂ H ₆ (89.5% Selectivity). C ₂ H ₄ (10.5% Selectivity)	Chen et al. (2016)
(7)	gas-liquid-solid system	UV lamp 254 nm	Pt/TiO ₂ 1.5 wt% Pt	0.075 g	CH ₄ 10 ml min ⁻¹	75 ml	1.6%	6 h	25°C	C ₂ H ₆ = 25 μmol CO ₂ = 35 μmol. H ₂ = 180 μmol	Yu et al. (2017)
(8)	Gas-liquid-solid system	UV lamp 254 nm	Pd/TiO ₂ (1.5 wt%)	0.075 g	CH ₄ 10 ml min ⁻¹	75 ml	1.0%	6 h	25°C	C ₂ H ₆ = 25 μmol CO ₂ = 10 μmol. H ₂ = 55 μmol	Yu and Li (2017)
(9)	Flow-type quartz reactor	Hg lamp 500 W	-TNT- Rh/TNT-Au/TNT-Au/TiO ₂	0.50 g	0.9 ml min ⁻¹ CH ₄ , 28.2 ml min ⁻¹ Ar (30 ml min ⁻¹), 0.9 ml min ⁻¹ water vapor stream	Vapor	-	-	403°K	Rh/TNT ₂ H ₂ = 296 μmol g ⁻¹ h ⁻¹ C ₂ H ₆ = 3.0 μmol g ⁻¹ h ⁻¹ CO ₂ = 41 μmol g ⁻¹ h ⁻¹	László et al. (2018)
(10)	Custom-made batch reactor 170 ml cell	300 W xenon lamp	Anatase TiO ₂ 0.12% Au/TiO ₂ 0.53% PdOx/TiO ₂ 0.69%	0.010 g	CH ₄ : Argon (1:19). 2 mM H ₂ O ₂ solution (4 ml)	6 ml	14.9%	3 h	25°C	FeO _x /TiO ₂ CH ₃ OH = 1,056 μmol gcat ⁻¹	Xie et al. (2018)

(Continued on following page)

TABLE 2 | (Continued) Methane conversion using metal-semiconductors as photocatalysts arranged in the order of publication year.

Entry	Reactor	Source	Photocatalyst	Photocatalyst amount	CH ₄ inlet	H ₂ O	CH ₄ conv	t	T	Products formed	References
(11)	Homemade stainless-steel batch reactor 230 ml	300 W Xe lamp equipped with a reflector	PtO/TiO ₂ , 0.29% Cu ₂ O/TiO ₂ 0.33% FeO _x /TiO ₂ Pt, Pd, Au, Ag 0.1% supported on ZnO and TiO ₂	0.010 g	0.1 MPa O ₂ 2 MPa CH ₄	100 ml	-	4 h	25°C	Au/ZnO CH ₃ OOH = 123.4 μmol CH ₃ OH = 41.2 μmol HCHO = 86.3 μmol CO = 0.4 μmol CO ₂ = 11.6 μmol C ₂ H ₄ = 686 μmol g ⁻¹ h ⁻¹	Song et al. (2019a)
(12)	100 ml micro autoclave	Xe lamp 84.2 mW/cm ²	0.3-1.5% Ag/TiO ₂	100 mg	CO ₂ /CH ₄ /Ar = 7.5/7.5/85 in terms of mole fraction) - pressure 2 MPa	-	-	2 h	-	CO = 1,149 μmol g ⁻¹ h ⁻¹ CO = 429 μmol g ⁻¹ h ⁻¹ CO ₂ = 85 μmol g ⁻¹ h ⁻¹	Li et al. (2019)
(13)	Homemade stainless-steel batch reactor 250 ml	Xe lamp 400 W	ZnHPV TiO ₂	0.10 g	CH ₄ 0.3 MPa Air 0.1 MPa	-	-	6 h	RT	CO = 429 μmol g ⁻¹ h ⁻¹ CO ₂ = 85 μmol g ⁻¹ h ⁻¹	Yu et al. (2019)
(14)	Photochemical reactor	Xe lamp 500 W	Cu -PCN	20 mg	CH ₄ 10 ml min ⁻¹ and N ₂ 90 ml min ⁻¹	25 ml	-	1 h	RT	C ₂ H ₅ OH = 21 μmol g ⁻¹ h ⁻¹ CH ₃ OH = 5.5 μmol g ⁻¹ h ⁻¹ C ₂ H ₆ = 13.9 μmol g ⁻¹ h ⁻¹ H ₂ = 7.0 μmol g ⁻¹ h ⁻¹ CO = 2.7 μmol g ⁻¹ h ⁻¹	Zhou et al. (2019)
(15)	Stainless-steel equipped with a quartz window (flow system)	365 nm light by a 40 W LED	Cu _x /PtTiO ₂	100 mg	O ₂ : CH ₄ = 1: 400 10% CH ₄	50 ml	-	-	RT	C ₂ H ₆ + C ₂ H ₄ (6.8 μmol h ⁻¹)	Li et al. (2020)
(16)	Homemade reactor	300 W Xe lamp with an AM 1.5G filter (100 mW cm ⁻²)	M/TiO ₂ (M = Au,Pt,Ir Ag,Pd,Rh,Ru)	5 mg deposited onto diffuse reflecting holder	10% CH ₄ in argon	-	-	-	RT	Au/TiO ₂ C ₂ H ₆ = 81.7 μmol g _{cat} ⁻¹ h ⁻¹	Lang et al. (2020)
(17)	Harrick reactor	White light illumination 19.2 W cm ⁻²	Cu-Ru/MgO-Al ₂ O ₃	~1.5 mg	CH ₄ 8 ml min ⁻¹ CO ₂ 8 ml min ⁻¹	-	275 μmol CH ₄ g ⁻¹ s ⁻¹	2 h	RT	CO: H ₂ (1:1)	Zhou et al. (2020)
(18)	33 ml custom-made tube reactor	300 W xenon lamp	Pd-modified Au/ZnO	2.0 mg dropped on conductive glass	0.5 ml of CH ₄	-	536 μmol CH ₄ g ⁻¹	8 h	RT	C ₂ H ₄ = 102.3 μmol g ⁻¹	Jiang et al. (2021)

phase revealed that the produced methanol competes with water molecules for the photogenerated holes and undergoes further decomposition. The authors concluded that the yield of methanol could be enhanced by its removal after formation. (Hameed et al., 2014).

Based on the fact that ordered mesoporous metal oxides showing large surface area and good light harvesting can result in efficient catalysts for many photocatalytic applications, La-doped mesoporous WO_3 was tested for the photocatalytic conversion of methane into methanol (Table 2, entry 5). La/ WO_3 was prepared in the following manner: a solution of LaNO_3 was added to the ethanolic solution of phosphotungstic acid hydrate (precursor of WO_3) and the resulting mixture was incorporated inside the host silica (KIT-6) that was further removed using HF. The photocatalytic activities of mesoporous WO_3 and La/ WO_3 were evaluated on the partial oxidation of methane to methanol with water under UVC-visible light irradiation at 55°C. The principal products formed were CH_3OH , C_2H_6 and CO_2 with minor quantities of H_2 , C_2H_4 , ethanol and formaldehyde. The photocatalyst La/ WO_3 produced more methanol and less amounts of C_2H_6 and CO_2 than pure WO_3 ; although appreciable amounts of CO_2 were produced for both catalysts. The superior performance of La/ WO_3 was mainly attributed to the formation of oxygen vacancies that increase H_2O adsorption and modification of basic-acid properties resulting in higher formation of $\bullet\text{OH}$ radicals (Villa et al., 2016).

Nanoparticulate ZnO exhibited exceptional activity under ultraviolet and UV-Vis light illumination as photocatalyst for CH_4 oxidation (Table 2, entry 6). For comparison purposes, the performance of commercial ZnO with particle sizes (200–300 μm) and TiO_2 P25 (benchmark photocatalyst), under the same conditions, exhibited mild and faint activity, respectively. Under visible light commercial ZnO and P25 showed no activity for CH_4 oxidation. On the other hand, nanoparticulate ZnO still shown significant activity and nano Ag decoration further enhanced the photoactivity *via* the surface plasmon resonance. The function of nano Ag decoration was attributed to: 1) as electron sink reducing the recombination of electrons and holes in the surface of ZnO and 2) as a photosensitizer extending the utilization of the visible light. A high quantum yield of 8% was observed at wavelengths <400 nm and only 0.1% at wavelengths \sim 470 nm. In the absence of oxygen, ethane was produced owing to the oxidative dehydrogenation of methane and, if ethane further abstracts hydrogen, the generation of ethylene may occur. In the flow mode under oxygen-free conditions a methane conversion of 0.35% and a selectivity of 89.47% for ethane was observed (Chen et al., 2016).

The direct combination of hydrogen evolution from water and methane conversion in a photocatalytic system was performed at 25°C using Pt nanoparticles supported on TiO_2 as photocatalysts, which were prepared by irradiation of UV light (254 nm) with different mass fraction of Pt (from 0.1 to 2%) (Table 2, entry 7). The activity of Pt/ TiO_2 photocatalysts increased with the increase of Pt content until 1.5% being H_2 , C_2H_6 and CO_2 the main products formed. For all cases, minor quantities of C_2H_4 and CO were also observed. The authors considered that the synergistic effect between the two reactions brings up the considerable

quantum efficiencies being 4.7% for H_2 production and 3.3% for CH_4 conversion. Thus, the synergistic effect of the addition of Pt on TiO_2 was an efficient way to improve the yields of both H_2 and C_2H_6 products due to the adequate utilization of photo-induced electron and holes, which contributed to the generation of H_2 and the conversion of CH_4 , respectively (Yu et al., 2017).

The direct combination of hydrogen evolution from water and methane conversion in a photocatalytic system was also performed using Pd/ TiO_2 with different Pd content (0.1–5 wt %) as photocatalysts (Table 2, entry 8). It was shown again that the efficient conversion of methane under ambient conditions and the photocatalytic splitting of water into H_2 could be introduced into one photocatalytic system achieving the simultaneous utilization of photo-induced electron and hole. Using only TiO_2 as photocatalyst the CH_4 conversion was very low and CO_2 was formed preferentially. The introduction of 0.1% of Pd improved H_2 production and the CH_4 conversion and C_2H_6 was preferentially formed. Increasing the Pd content (0.5, 1 and 1.5%) the H_2 production and the CH_4 conversion also increased, together with increasing of C_2H_6 and a little increasing of CO_2 . More additions of Pd (2, 3 and 5%) practically do not increase the H_2 production and CH_4 conversion. Thus, the addition of Pd changed the selectivity of the production of C_2H_6 and CO_2 , but amounts above 1.5% of Pd barely vary the selectivity (the highest was 72.6%). Considering the desired product (C_2H_6) 1.5%-Pd/ TiO_2 was considered as the best photocatalyst. It was determined that the photo-induced electron was used mostly for the production of H_2 , while the hole was used for the conversion of CH_4 . In this manner, the photoinduced electrons and holes can be effectively separated and adequately utilized providing a new strategy for photocatalytic reaction, and brought up considerable quantum efficiencies, which is still low (ca. 5%). The Pd/ TiO_2 catalyst showed excellent property in this novel synergistic photocatalytic pathway between H_2 production from water and coupling of CH_4 to ethane. The $\bullet\text{CH}_3$ radical was demonstrated to play an important role the forming of C_2H_6 , being the highest selectivity reaching 72.6%. The authors considered that the work provided a new strategy for photocatalytic reaction improving the quantum efficiencies for electron of 2.83% and for hole of 2.76% (Yu and Li, 2017).

The photocatalytic conversion of methane was studied on titanate nanotubes (TNT) and TiO_2 anatase modified with Au and Rh nanoparticles (Table 2, entry 9). Rh/TNT (average Rh nanoparticles 2.8 nm, band gap 3.08 eV) and Au/ TiO_2 (average Au nanoparticles 7.4 nm, band gap 3.04 eV) were prepared by incipient wetness impregnation and the metals were reduced using H_2 . Au/TNT (average Au nanoparticles 3.1 nm, band gap 3.03 eV) was prepared using NaBH_4 solution as reducing agent. The photocatalysts were tested using a CH_4 - H_2O -Ar mixture (CH_4 : H_2O = 1:1 M ratio). The products formed were H_2 , C_2H_6 , CO_2 , CO and CH_3OH . In the photocatalytic tests experiments it was observed that the pure TNT support showed low activity in CH_4 conversion and the addition of metal significantly increased the rate of CH_4 consumption. The order of methane conversion was Rh/TNT > Au/ TiO_2 > AuTNT \sim TiO_2 . The formation of hydrogen followed the same tendency with Rh/TNT producing

296 $\mu\text{mol g}_{\text{cat}}^{-1} \text{h}^{-1}$. The major quantities of ethane production (5.8 $\mu\text{mol g}_{\text{cat}}^{-1} \text{h}^{-1}$) were obtained using TiO_2 and Au/TiO_2 photocatalysts showing that the deposition of Au on TiO_2 did not increase the rate of ethane formation. However, the quantity of H_2 produced on Au/TiO_2 (191 $\mu\text{mol g}_{\text{cat}}^{-1} \text{h}^{-1}$) was greater than the TiO_2 (3.8 $\mu\text{mol g}_{\text{cat}}^{-1} \text{h}^{-1}$) support (László et al., 2018).

Au/TiO_2 , $\text{PdO}_x/\text{TiO}_2$, PtO/TiO_2 , $\text{Cu}_2\text{O/TiO}_2$ and $\text{FeO}_x/\text{TiO}_2$ prepared by impregnation and calcination at 400°C were evaluated for the conversion of methane to methanol at room temperature under moderate light irradiation (close to one Sun) in the presence of H_2O_2 (Table 2, entry 10). The samples prepared with noble metals (Au, Pd and Pt) showed lower CH_4 conversions compared to bare TiO_2 support being the main product CO_2 . The photocatalyst $\text{FeO}_x/\text{TiO}_2$ exhibited an increase of 1.5 times for CH_4 conversion enhancing methanol production by around four times when compared to pure TiO_2 . The methane conversion achieved 14.9% after 3 h of reaction. The yield was 1,056 $\mu\text{mol g}_{\text{cat}}^{-1}$, that correspond to 18 mol of methanol per mole of Fe. The superior activity of the $\text{FeO}_x/\text{TiO}_2$ photocatalyst at ambient conditions was attributed to the efficient electron transfer from TiO_2 to iron species, a lower overpotential for H_2O_2 reduction on iron species and suppression of the oxygen reduction reaction that would change the selectivity to CO_2 , decreasing methanol formation (Xie et al., 2018).

Pt, Pd, Au and Ag (0.1 wt%) loaded on ZnO and TiO_2 were prepared by borohydride reduction method and tested in the photocatalytic methane oxidation reaction at room temperature in the presence of water and under 2 MPa CH_4 and 0.1 MPa O_2 (Table 2, entry 11). Among all photocatalysts Au/ZnO showed superior performance leading to the formation of methyl hydroperoxide, methanol and formaldehyde as the main products with minor quantities of CO_2 when compared to others photocatalysts. The efficient oxidation of methane was attributed to the powerful ability of noble metal/ZnO photocatalysts to activate simultaneously CH_4 and O_2 molecules in aqueous solution generating $\bullet\text{CH}_3$ and $\bullet\text{OOH}$ radicals through of holes and electrons, which lead to the formation of oxygenates liquid products. Conducting experiments using isotopically labeled oxygen and water revealed that molecular O_2 was the source of oxygen for direct CH_4 oxidation (Song et al., 2019a).

The photocatalytic oxidative coupling of methane under mild conditions was performed using CO_2 as oxidant and Ag/TiO_2 (0.3, 0.5, 1.0 and 1.5% Ag) as photocatalysts prepared by borohydride reduction (Table 2, entry 12). The reaction was carried out in a microautoclave under 2 MPa of pressure in the presence of sunlight. Blank experiment without adding catalyst or in the absence of light showed no products. Using bare TiO_2 as photocatalyst only a small quantity of CO was detected while the addition of Ag (1 wt%) resulted in the production of 1.149 $\mu\text{mol g}_{\text{cat}}^{-1} \text{h}^{-1}$ of CO and 686 $\mu\text{mol g}_{\text{cat}}^{-1} \text{h}^{-1}$ of C_2H_4 . In order to understanding the photocatalytic process further experiments were performed and it was concluded that the performance was a result of the synergy of visible-light inducing Ag LSPR effect and UV-light induced TiO_2 photoexcitation effect, as well as the preferential adsorption of CO_2 on TiO_2 and CH_4 on Ag (Li et al., 2019).

The direct selective photocatalytic conversion of methane into carbon monoxide with only small quantities of CO_2 was performed in a batch reactor with a quartz window under 0.3 MPa of CH_4 and 0.1 MPa of air at room temperature (Table 2, entry 13). The photocatalysts used were noble or transition metals ($M = \text{Ag, Pd, V, Fe, Ga, Ce, Co, Cu}$ and Zn) species highly dispersed on tungstophosphoric acid, which was dispersed as a thin layer of 1–2 nm over titanium oxide ($M\text{-HPW/TiO}_2$). In the absence of light no products were observed for all photocatalysts. Using HPW, TiO_2 and HPW/TiO_2 as photocatalysts the production of CO and CO_2 were very low, being CO_2 preferentially formed. Among the $M\text{-HPW/TiO}_2$ photocatalysts the material containing Zn showed the best performance producing 429 $\mu\text{mol g}^{-1} \text{h}^{-1}$ of CO and 85 $\mu\text{mol g}^{-1} \text{h}^{-1}$ of CO_2 (CO selectivity of 84%). *In-situ* FTIR and XPS suggested that the catalytic performance could be attributed to zinc species highly dispersed on HPW/TiO_2 , which undergo reduction and oxidation cycles during the reaction and the reaction proceeds *via* intermediate formation of methyl carbonates (Yu et al., 2019).

The direct functionalization of methane into ethanol *via* photocatalysis was reported over Cu modified polymeric carbon nitride (Cu-PCN) (Table 2, entry 14). The Cu-PCN photocatalysts were prepared by dissolution of urea and copper chloride in water and after this, the solution was evaporated resulting in a slurry that was treated at 550°C in air. Blanks experiments revealed that no products were formed without photocatalysts or without methane. Using 20 mg Cu-PCN as photocatalysts in the presence of CH_4 and H_2O the following quantities of products were observed after 1 h: $\text{C}_2\text{H}_5\text{OH} = 21 \mu\text{mol g}^{-1} \text{h}^{-1}$, $\text{CH}_3\text{OH} = 5.5 \mu\text{mol g}^{-1} \text{h}^{-1}$, $\text{C}_2\text{H}_6 = 13.9 \mu\text{mol g}^{-1} \text{h}^{-1}$, $\text{H}_2 = 7.0 \mu\text{mol g}^{-1} \text{h}^{-1}$ and $\text{CO} = 2.7 \mu\text{mol g}^{-1} \text{h}^{-1}$. The authors considered that despite the conduction band of Cu/PCN was suitable for H_2 evolution, no H_2 was detected in the methane-free experiment thus excluding H_2O splitting. They consider that Cu-PCN could manage the generation of H_2O_2 and its decomposition to produce $\bullet\text{OH}$ radicals, of which Cu species were also active sites for methane adsorption and activation. This avoided excess $\bullet\text{OH}$ radicals for over-oxidation and facilitated methane conversion (Zhou et al., 2019).

A continuous photocatalytic oxidative coupling of methane at room temperature and atmospheric pressure was described in a flow system reactor (Table 2, entry 15). The Pt and CuO_x -decorated TiO_2 photocatalyst denoted as CuPt/TiO_2 was prepared first introducing Pt by photodeposition and then Cu was incorporated by wet impregnation method. The photocatalysts were prepared with different quantities of Pt and Cu. The optimized $\text{Cu}_{0.1}\text{Pt}_{0.5}/\text{TiO}_2$ photocatalyst showed the highest yield (6.8 $\mu\text{mol h}^{-1}$) of C_2 products (ethane and ethene, ethane selectivity >90%), which was greater than the obtained with Pt/TiO_2 (1.07 $\mu\text{mol h}^{-1}$) and Cu/TiO_2 (1.9 $\mu\text{mol h}^{-1}$). On the other hand, CO_2 was also formed on these reactions and about 7.5 $\mu\text{mol h}^{-1}$ was obtained using bare TiO_2 , while in the presence of $\text{Cu}_{0.1}\text{Pt}_{0.5}/\text{TiO}_2$ its quantity increased only 20% (~9 $\mu\text{mol h}^{-1}$). The authors proposed that upon light irradiation electrons were excited from VB of TiO_2 to its CB and then migrate to Pt, while holes could be transferred to the VB

of CuO_x retarding their recombination and lowering the oxidation potential of photoinduced holes to avoid deep dehydrogenation and over-oxidation. Thus, C–H bond of methane molecules were broken by the holes in the VB of CuO_x species to form methyl radicals that combining forming ethane molecules. The O_2 were reduced by electrons from Pt sites to form the superoxide anion radical ($\text{O}_2^{\bullet-}$) that react with protons forming H_2O (Li et al., 2020).

The non-oxidative coupling of methane was studied using M/TiO₂ (M = Au, Ru, Rh, Pd, Ag, Ir and Pt) as photocatalysts, which were prepared through a photodeposition method (Table 2, entry 16). The reactions were performed in a continuous-flow photocatalytic system. No hydrocarbon products were detected for the NOCM process without light irradiation or replacing CH_4 by argon even under light irradiation. In the presence of TiO₂ the methane conversion was very low. In contrast, all M/TiO₂ photocatalysts were active under light irradiation showing the following order of activity: Au > Ag > Ru > Pd > Ir > Pt > Rh producing 16.3 > 5.2 > 4.3 > 4.2 > 1.9 > 0.8 mmol_{C₂H₆} g_{metal}⁻¹ h⁻¹, respectively. Among all photocatalysts, Au/TiO₂ showed the best performance yielding 81.7 μmol g_{cat}⁻¹ h⁻¹ without the addition of H_2O or any other oxidants. C_3H_8 was also produced over Au/TiO₂, but the yield was very small. The equimolar amount of H_2 :ethane of 1:1 was produced over Au/TiO₂. The best performance was attributed to the easy transport of photoelectrons from TiO₂ to Au inhibiting the photoelectron-hole recombination. *In situ* FTIR measurements and DFT calculations revealed that CH_4 was transformed into methyl radicals to form ethane via a methyl anion activation process (Lang et al., 2020).

The methane dry reforming ($\text{CH}_4 + \text{CO}_2 \rightarrow 2\text{CO} + 2\text{H}_2$) at room temperature was performed using as photocatalysts Cu-Ru/MgO-Al₂O₃ prepared with different Cu-Ru loadings by coprecipitation (Table 2, entry 17). For pure Cu nanoparticles the initial reaction rate was approximately 50 μmol CH_4 g⁻¹ s⁻¹, however when an extremely low fraction of Ru (Cu_{19.95}Ru_{0.05}) was added, the reaction rate increased 2.5 times (128 μmol CH_4 g⁻¹ s⁻¹) and the H_2 /CO selectivity value increased to 0.8. Slightly increasing the Ru loading to 0.1 and 0.2 resulted in an increase of reaction rates (between 200 and 275 μmol CH_4 g⁻¹ s⁻¹) and H_2 /CO selectivity values were close to 1. Increasing the Ru loading to 0.5 although the activity increased, the selectivity values decreased. The substantial differences in the photocatalytic activity with different Ru quantities (from 0.05 to 0.50) was attributed to monodispersed Ru atoms (single-atom) on the Cu nanoparticle. It was proposed light-excited hot carriers together with single-atom active sites cause the observed performance, that is, the small plasmonic Cu provide strong light absorption generating hot carriers under illumination, while single-atom Ru sites on the Cu surface offer high catalytic activity (Zhou et al., 2020).

Recently, a photocatalytic conversion of methane to ethylene under mild conditions was reported using AuPd/ZnO nanoporous as photocatalysts prepared by depositing pre-synthesized AuPd core-shell nanorods on the porous of ZnO (Table 2, entry 18). Au nanorods were chosen as the plasmonic metal nanostructure and Pd was selected as a modifier to

modulate the dehydrogenation capability to improve C_2H_4 selectivity. Using pure ZnO as photocatalyst practically no products were formed. Au/ZnO and Pd/ZnO showed low activity and C_2H_4 selectivity; however, introducing Pd into the lattice of Au the photocatalytic performance and especially C_2H_4 selectivity increased strongly. As a result, a methane conversion of 536 μmol g⁻¹ and a C_2^+ compounds selectivity of 96% (39.7% C_2H_4 and 54.9% C_2H_6 in total produced C_2^+ compounds) was obtained using the optimized AuPd_{2.7%}/ZnO photocatalyst after 8 h of irradiation. Based on *in situ* characterizations, it was revealed that methane molecules were first dissociated into methoxy on the surface of ZnO under the assistance of Pd and the methoxy intermediates were further dehydrogenated and coupled with methyl radical into ethoxy, which were subsequently converted into ethylene through dehydrogenation (Jiang et al., 2021).

Analyzing the data in Tables 1, 2 it could be seen that the products formed in the photocatalytic conversion of methane are greatly influenced by the conditions under which the reactions are carried out, such as:

- 1) *In the presence of O_2 or the use of oxidizing agent like H_2O_2* : the oxygenated products like CH_3OH , HCOOH , CH_3COH , CH_3OOH , HCHO , CO and CO_2 were formed (Table 1, entries 4 and 6 and Table 2, entries 10, 11 and 13).
- 2) *In the absence of water and oxygen*: the non-oxidative coupling of methane reaction was favored forming C_2H_6 and C_2H_4 (Table 1, entries 1 and 2 and Table 2, entries 3, 6, 16 and 18).
- 3) *In the presence of water and absence of oxygen*: a greater diversity of products such as CH_3OH , CH_3CHO , $\text{CH}_3\text{CH}_2\text{OH}$, C_2H_6 , CO , CO_2 and H_2 could be formed (Table 1, entries 3 and 5 and Table 2, entries 1, 2, 4, 5, 7, 8, 9 and 14). The advantage of carrying out the reaction in the presence of water is that the evolution of hydrogen can be combined with the conversion of methane (Table 2, entries 4, 7, 8, 9).
- 4) *In the presence of CO_2* : the formation of C_2H_4 and CO through the oxidative coupling of methane was described, where CO_2 works as an oxidizing agent (Table 2, entry 12) and the formation of syn gas CO : H_2 (1:1) by dry reforming of methane (Table 2, entry 17).

Another important point is that the use of different photocatalysts affect the methane conversion and the selectivity of the products formed when the reaction are carried out under similar conditions. For example, see Table 2, entries 7, 8 and 9, where the reactions were performed in the presence of water and absence of oxygen using Pt/TiO₂, Pd/TiO₂ and Rh/TNT photocatalysts, respectively. In these reactions, the products formed for all photocatalysts were C_2H_6 , CO_2 and H_2 , however, the methane conversions and products selectivity were different. Another example is observed for reactions performed in the absence of water and oxygen (Table 2, entries 16 and 18) where the Au/TiO₂ and Pd-Au/TiO₂ photocatalysts were more selective for the production of C_2H_6 or C_2H_4 . Also, some reactions were favored using different photocatalysts, for instance, the

reactions carried out in the presence of CO₂ using the same CH₄:CO₂ molar ratio of 1:1 (Table 2, entries 12 and 17). The oxidative coupling of methane was favored using Ag/TiO₂ as photocatalyst (Table 2, entry 12) and dry reforming of methane using Cu-Ru/MgO-Al₂O₃ photocatalyst (Table 2, entry 17). On the other hand, it should be noted that the activities of the photocatalysts for methane conversion are still quite low ($\mu\text{mol g}^{-1} \text{h}^{-1}$). Thus, due to the different conditions used in these reactions (type of reactor, light source, etc.) and techniques for detection and quantification of the products formed, a quantitative comparison of these data may not be very accurate.

CONCLUSIONS AND PERSPECTIVES

Studies on the photocatalytic conversion of methane at low temperatures have attracted the attention of the scientific community in recent years with the objective of the production of more valuable products (ethane, ethylene, methanol, CO, hydrogen) reducing the energy consumption and the environmental impacts. The photocatalysts that have been most used in these reactions are semiconductors like TiO₂, ZnO, Ga₂O₃ and WO₃ and hybrid metal-semiconductor materials, where metals like Pt, Pd, Au, Ag, Cu and Fe have been the most used. The most studied reactions are the oxidative and non-oxidative coupling of methane, the direct conversion of methane to methanol and steam and dry reforming of methane. It is important to point out the difficulty in establishing proper comparisons among the various works since the operational conditions used are very different (light source, pressure, reactor-type, etc.). In addition, studies of stability and deactivation of photocatalysts are also absent in most works. The combination of metal and semiconductor has proved to be a

good strategy to develop more active photocatalysts. This is basically due to the improvement of charge separation (photoelectrons and holes) pulping the electrons to surface for reaction, the activation of methane by metals and the plasmon resonance effect of some metals. Therefore, the development of more active photocatalysts should take into account the increase in light absorption (mainly in the visible region), the separation of charges and the surface reactions. This involves some strategies and methods to control the composition, sizes and morphologies of the metals and the semiconductors, the doping of the semiconductors and the interactions between them, for instance, depositing metals on specific facets of the semiconductor, joining semiconductors to facilitate the separation of photogenerated charge carriers, etc. The metal organic framework (MOF) has the property of adsorbing large amounts of methane and, therefore, can be an interesting for developing hybrid photocatalysts for methane conversion (Shah et al., 2020). However, although the knowledge in this area has advanced, the possibilities of combinations are endless and there is a plenty of room to be investigated and improved.

AUTHOR CONTRIBUTIONS

All authors listed have made a substantial, direct, and intellectual contribution to the work and approved it for publication.

FUNDING

We acknowledge financial support and fellowships from CINE - SHELL (ANP)/FAPESP grants n° 2017/11937-4, 2018/04596-9 and 2018/04595-2. CNPq (305622/2020-0) is also acknowledged.

REFERENCES

- Chen, X., Li, Y., Pan, X., Cortie, D., Huang, X., and Yi, Z. (2016). Photocatalytic Oxidation of Methane over Silver Decorated Zinc Oxide Nanocatalysts. *Nat. Commun.* 7, 1–8. doi:10.1038/ncomms12273
- Du, J., Chen, W., Wu, G., Song, Y., Dong, X., Li, G., et al. (2020). Evoked Methane Photocatalytic Conversion to C2 Oxygenates over Ceria with Oxygen Vacancy. *Catalysts* 10, 196. doi:10.3390/catal10020196
- Gao, Y., Neal, L., Ding, D., Wu, W., Baroi, C., Gaffney, A. M., et al. (2019). Recent Advances in Intensified Ethylene Production-A Review. *ACS Catal.* 9, 8592–8621. doi:10.1021/acscatal.9b02922
- Hameed, A., Ismail, I. M. I., Aslam, M., and Gondal, M. A. (2014). Photocatalytic Conversion of Methane into Methanol: Performance of Silver Impregnated WO₃. *Appl. Catal. A: Gen.* 470, 327–335. doi:10.1016/j.apcata.2013.10.045
- Horn, R., and Schlögl, R. (2015). Methane Activation by Heterogeneous Catalysis. *Catal. Lett.* 145, 23–39. doi:10.1007/s10562-014-1417-z
- Jiang, W., Low, J., Mao, K., Duan, D., Chen, S., Liu, W., et al. (2021). Pd-Modified ZnO-Au Enabling Alkoxy Intermediates Formation and Dehydrogenation for Photocatalytic Conversion of Methane to Ethylene. *J. Am. Chem. Soc.* 143, 269–278. doi:10.1021/jacs.0c10369
- Kato, Y., Yoshida, H., and Hattori, T. (1998). Photoinduced Non-oxidative Coupling of Methane over Silica-Alumina and Alumina Around Room Temperature. *Chem. Commun.*, 2389–2390. doi:10.1039/A806825I
- Lang, J., Ma, Y., Wu, X., Jiang, Y., and Hu, Y. H. (2020). Highly Efficient Light-Driven Methane Coupling under Ambient Conditions Based on an Integrated Design of a Photocatalytic System. *Green. Chem.* 22, 4669–4675. doi:10.1039/d0gc01608j
- László, B., Baán, K., Oszkó, A., Erdöhelyi, A., Kiss, J., and Kónya, Z. (2018). Hydrogen Evolution in the Photocatalytic Reaction between Methane and Water in the Presence of CO₂ on Titanate and Titania Supported Rh and Au Catalysts. *Top. Catal.* 61, 875–888. doi:10.1007/s11244-018-0936-z
- Li, L., Cai, Y.-Y., Li, G.-D., Mu, X.-Y., Wang, K.-X., and Chen, J.-S. (2012). Synergistic Effect on the Photoactivation of the Methane C-H Bond over Ga³⁺-Modified ETS-10. *Angew. Chem. Int. Ed.* 51, 4702–4706. doi:10.1002/anie.201200045
- Li, N., Jiang, R., Li, Y., Zhou, J., Ma, Q., Shen, S., et al. (2019). Plasma-Assisted Photocatalysis of CH₄ and CO₂ into Ethylene. *ACS Sustain. Chem. Eng.* 7, 11455–11463. doi:10.1021/acssuschemeng.9b01284.s001
- Li, X., Xie, J., Rao, H., Wang, C., and Tang, J. (2020). Platinum and CuO X Decorated TiO₂ Photocatalyst for Oxidative Coupling of Methane to C₂ Hydrocarbons in a Flow Reactor. *Angew. Chem. Int. Ed.* 59, 19702–19707. doi:10.1002/anie.202007557
- Liu, L., Zhang, X., Yang, L., Ren, L., Wang, D., and Ye, J. (2017). Metal Nanoparticles Induced Photocatalysis. *Natl. Sci. Rev.* 4, 761–780. doi:10.1093/nsr/nwx019
- Murcia-López, S., Bacariza, M. C., Villa, K., Lopes, J. M., Henriques, C., Morante, J. R., et al. (2017). Controlled Photocatalytic Oxidation of Methane to Methanol through Surface Modification of Beta Zeolites. *ACS Catal.* 7, 2878–2885. doi:10.1021/acscatal.6b03535
- Olivos-Suarez, A. I., Szécsényi, Á., Hensen, E. J. M., Ruiz-Martinez, J., Pidko, E. A., and Gascon, J. (2016). Strategies for the Direct Catalytic Valorization of

- Methane Using Heterogeneous Catalysis: Challenges and Opportunities. *ACS Catal.* 6, 2965–2981. doi:10.1021/acscatal.6b00428
- Reddy, N. L., Rao, V. N., Vijayakumar, M., Santhosh, R., Anandan, S., Karthik, M., et al. (2019). A Review on Frontiers in Plasmonic Nano-Photocatalysts for Hydrogen Production. *Int. J. Hydrogen Energ.* 44, 10453–10472. doi:10.1016/j.ijhydene.2019.02.120
- Sher Shah, M. S. A., Oh, C., Park, H., Hwang, Y. J., Ma, M., and Park, J. H. (2020). Catalytic Oxidation of Methane to Oxygenated Products: Recent Advancements and Prospects for Electrocatalytic and Photocatalytic Conversion at Low Temperatures. *Adv. Sci. (Weinh)* 7, 2001946. doi:10.1002/advs.202001946
- Shimura, K., Yoshida, T., and Yoshida, H. (2010). Photocatalytic Activation of Water and Methane over Modified Gallium Oxide for Hydrogen Production. *J. Phys. Chem. C* 114, 11466–11474. doi:10.1021/jp1012126
- Song, H., Meng, X., Wang, S., Zhou, W., Wang, X., Kako, T., et al. (2019a). Direct and Selective Photocatalytic Oxidation of CH₄ to Oxygenates with O₂ on Cocatalysts/ZnO at Room Temperature in Water. *J. Am. Chem. Soc.* 141, 20507–20515. doi:10.1021/jacs.9b11440
- Song, H., Meng, X., Wang, Z.-j., Liu, H., and Liu, J. (2019b). Solar-Energy-Mediated Methane Conversion. *Joule* 3, 1606–1636. doi:10.1016/j.joule.2019.06.023
- Takanabe, K. (2019). Addressing Fundamental Experimental Aspects of Photocatalysis Studies. *J. Catal.* 370, 480–484. doi:10.1016/j.jcat.2018.10.006
- Tang, P., Zhu, Q., Wu, Z., and Ma, D. (2014). Methane Activation: the Past and Future. *Energy Environ. Sci.* 7, 2580–2591. doi:10.1039/c4ee00604f
- Taylor, C. E. (2003). Methane Conversion via Photocatalytic Reactions. *Catal. Today* 84, 9–15. doi:10.1016/S0920-5861(03)00295-5
- Villa, K., Murcia-López, S., Morante, J. R., and Andreu, T. (2016). An Insight on the Role of La in Mesoporous WO₃ for the Photocatalytic Conversion of Methane into Methanol. *Appl. Catal. B: Environ.* 187, 30–36. doi:10.1016/j.apcatb.2016.01.032
- Wei, J., Yang, J., Wen, Z., Dai, J., Li, Y., and Yao, B. (2017). Efficient Photocatalytic Oxidation of Methane over β -Ga₂O₃/activated Carbon Composites. *RSC Adv.* 7, 37508–37521. doi:10.1039/c7ra05692c
- Wu, S., Wang, L., and Zhang, J. (2021). Photocatalytic Non-oxidative Coupling of Methane: Recent Progress and Future. *J. Photochem. Photobiol. C: Photochem. Rev.* 46, 100400. doi:10.1016/j.jphotochemrev.2020.100400
- Xie, J., Jin, R., Li, A., Bi, Y., Ruan, Q., Deng, Y., et al. (2018). Highly Selective Oxidation of Methane to Methanol at Ambient Conditions by Titanium Dioxide-Supported Iron Species. *Nat. Catal.* 1, 889–896. doi:10.1038/s41929-018-0170-x
- Yoshida, H., Kato, S., Hirao, K., Nishimoto, J.-i., and Hattori, T. (2007). Photocatalytic Steam Reforming of Methane over Platinum-Loaded Semiconductors for Hydrogen Production. *Chem. Lett.* 36, 430–431. doi:10.1246/cl.2007.430
- Yu, L., and Li, D. (2017). Photocatalytic Methane Conversion Coupled with Hydrogen Evolution from Water over Pd/TiO₂. *Catal. Sci. Technol.* 7, 635–640. doi:10.1039/C6CY02435A
- Yu, L., Shao, Y., and Li, D. (2017). Direct Combination of Hydrogen Evolution from Water and Methane Conversion in a Photocatalytic System over Pt/TiO₂. *Appl. Catal. B: Environ.* 204, 216–223. doi:10.1016/j.apcatb.2016.11.039
- Yu, X., De Waele, V., Löfberg, A., Ordonsky, V., and Khodakov, A. Y. (2019). Selective Photocatalytic Conversion of Methane into Carbon Monoxide over Zinc-Heteropolyacid-Titania Nanocomposites. *Nat. Commun.* 10, 700. doi:10.1038/s41467-019-08525-2
- Yuliati, L., Hattori, T., Itoh, H., and Yoshida, H. (2008a). Photocatalytic Nonoxidative Coupling of Methane on Gallium Oxide and Silica-Supported Gallium Oxide. *J. Catal.* 257, 396–402. doi:10.1016/j.jcat.2008.05.022
- Yuliati, L., Itoh, H., and Yoshida, H. (2008b). Photocatalytic Conversion of Methane and Carbon Dioxide over Gallium Oxide. *Chem. Phys. Lett.* 452, 178–182. doi:10.1016/j.cplett.2007.12.051
- Yuliati, L., and Yoshida, H. (2008). Photocatalytic Conversion of Methane. *Chem. Soc. Rev.* 37, 1592–1602. doi:10.1039/b710575b
- Zeng, Y., Liu, H. C., Wang, J. S., Wu, X. Y., and Wang, S. L. (2020). Synergistic Photocatalysis-Fenton Reaction for Selective Conversion of Methane to Methanol at Room Temperature. *Catal. Sci. Technol.* 10, 2329–2332. doi:10.1039/d0cy00028k
- Zeng, Z.-Y., Chen, J., and Lin, J.-H. (2018). Unexpectedly Promoting Effect of Carbon Nanotubes Grown during the Non-oxidative Coupling of Methane over Copper Catalysts. *Front. Res. Today* 1, 1007. doi:10.31716/frt.201801007
- Zhou, L., Martirez, J. M. P., Finzel, J., Zhang, C., Swearer, D. F., Tian, S., et al. (2020). Light-driven Methane Dry Reforming with Single Atomic Site Antenna-Reactor Plasmonic Photocatalysts. *Nat. Energ.* 5, 61–70. doi:10.1038/s41560-019-0517-9
- Zhou, Y., Zhang, L., and Wang, W. (2019). Direct Functionalization of Methane into Ethanol over Copper Modified Polymeric Carbon Nitride via Photocatalysis. *Nat. Commun.* 10. doi:10.1038/s41467-019-08454-0

Conflict of Interest: The authors declare that the research was conducted in the absence of any commercial or financial relationships that could be construed as a potential conflict of interest.

Copyright © 2021 Januario, Silvaino, Machado, Moreira Vaz and Spinace. This is an open-access article distributed under the terms of the Creative Commons Attribution License (CC BY). The use, distribution or reproduction in other forums is permitted, provided the original author(s) and the copyright owner(s) are credited and that the original publication in this journal is cited, in accordance with accepted academic practice. No use, distribution or reproduction is permitted which does not comply with these terms.